HOT FORMABILITY CHARACTERIZATION AND FRACTURE LOCUS DETERMINATION OF THE CuZn40Pb2 BRASS ALLOY THROUGH TENSILE AND TORSION TESTING

S. BRUSCHI*, A. GHIOTTI* AND M. F. NOVELLA*

* Dipartimento di Ingegneria Industriale (DII)
Università degli Studi di Padova
Via Venezia 1, 35131, Padova, Italy
e-mail: stefania.bruschi@unipd.it, andrea.ghiotti@unipd.it,
michele.novella@studenti.unipd.it, www.dii.unipd.it

Key words: metal forming, forging, formability, damage, triaxiality,

Abstract. The prediction of ductile fracture occurrence in hot forging processes is one of the main industrial issues, which needs damage models that have to be on one hand accurate and easily calibrated, but also easy enough to be industrially implemented an utilized.

Tensile testing formability characterization, although experimentally easy, does not allow taking into account all the variables influencing the evolution of damage, making the calibration test-dependent. Besides the stress triaxiality factor effect, in hot forging processes, the stress deviatoric parameter, the temperature and strain rate must be taken into account to provide reliable and efficient models.

In this work hot fracture characterization was performed on the dual-phase brass alloy CuZn40Pb2, typically used for hot forging and characterized by a narrow temperature window of formability. The values of true strain at fracture from tensile, torsion and tensile-torsion tests performed at various temperatures and strain rates are obtained. Numerical simulations of the above-cited tests were carried out in order to determine the three-dimensional surfaces of the fracture locus as a function of the stress triaxiality and deviatoric parameter.

The results are critically discussed and in particular the influence of the rheological behaviour of the material on the fracture locus shape is highlighted.

Optical microscopy analysis was carried out in order to assess the testing parameters influence on the phase distribution and EDS-SEM analysis to evaluate the grain boundary composition, which was recognized critical as regards the formability characteristics of the investigated alloy.

1 INTRODUCTION

Metal formability is a key parameter in order to attain effective net shape or near-to-net-shape in bulk metal forming processes, since an accurate fracture prediction allows the design of more efficient process chains in terms of number of forging steps and dies geometries,

resulting in more dimensionally accurate forged parts at lower production costs.

Ductile fracture prediction in bulk deformation processes has been an issue widely faced by means of ductile fracture criteria, which are encountering more and more interest in the industrial world due to more reliable and user-friendly software tools and increased computing devices.

Two approaches are essentially adopted ain literature: the empirical fracture criteria and the Continuum Damage Mechanics criteria. The former includes a wide series of fracture criteria such as Cockroft and Latham's, Rice and Tracey's and Oyane's ones [1, 2, 3]. Their analytical formulation appears simple as well as their experimental calibration, but the damage evolution is not coupled with the rheological characteristics of the material and the calibration is test-dependent: the less similar the calibration and validation conditions are, the less reliable the fracture predictions usually proves to be. The latter [4], on the other hand, offers a fully coupled modelling of the damage evolution and the mechanical behaviour of the material, allowing a theoretically test-independent experimental calibration. Despite this, the experimental calibration is expensive and the analytical complexity of this approach results in a not easy FE implementation, keeping this approach limited to scientific applications.

Moreover the ductile damage criteria have historically been developed to describe damage evolution and predict crack onset in cold deformation processes: while the extension to hot processes of the Continuum Damage Mechanics is possible, due to the dependence of the model constants on temperature, the empirical criteria do not take into account in any way the temperature and strain rate effect.

In more recent studies [5, 6] the effect of the deviatoric parameter X on material equivalent strain at fracture has been highlighted. The definition of X is given in equation (1), where $\bar{\sigma}$ is the Von Mises equivalent stress, while J_3 is the third invariant of the deviatoric component of the stress tensor.

$$X = \frac{27}{2}\frac{J_3}{\bar{\sigma}^3} \tag{1}$$

It was also recognized [7, 8] that equivalent strain at fracture as a function of stress triaxiality factor T has exponential lower and upper limits corresponding to two constant values of the deviatoric parameter: the lower limit (X=0) represents the plane strain condition, while the upper one (X=1) corresponds to axisymmetric stress state.

Under the Tresca hypothesis [9] the equivalent strain at fracture can be expressed as a function of the upper limit, X, T and n, the strain hardening coefficient of the material, as shown in equation (2):

$$\bar{\varepsilon}_f = \bar{\varepsilon}_{f,1}\left[\frac{sin\left(\frac{\pi}{3}\right)}{sin\left(\frac{2\pi - \arccos(X)}{3}\right)}\right]^{\frac{1}{n}} = C_1 e^{-C_2 T}\left[\frac{sin\left(\frac{\pi}{3}\right)}{sin\left(\frac{2\pi - \arccos(X)}{3}\right)}\right]^{\frac{1}{n}} \tag{2}$$

Equation (2), plotted in the X-T domain, gives a 3D surface describing the fracture locus of the material. This kind of approach leads to the formulation of a ductile damage law [9],

whose experimental calibration appears reasonably simple, since it only needs tensile tests with notched specimen of different geometries for calibration and a simple torsion test to have a first validation. The main advantage of such an approach is that the material formability is described as a function of *X* and *T*, which are sufficient to give a complete characterization of the stress tensor. This, in turn, implies a more general damage model, which keeps into account the shape of the stress tensor, leading to a test-independent calibration.

The aim of this work is to extend the application of this approach to the hot processes field, assessing the reliability of the model at high temperatures and the fracture locus shape. The reference material used is the dual-phase brass alloy CuZn40Pb2, typically used for hot forging and characterized by a narrow temperature window of formability. In particular the industrial process taken as reference is the hot forging of a torx-type screw.

Hot compression tests were carried out to determine the mechanical characteristics of this alloy to be implemented in Forge 2011^{TM} FE code. In order to determine the upper formability limit, tensile tests on notched specimens of different geometries were carried out to assess equivalent strain at fracture of the material at different triaxiality levels, evaluated by means of FE simulations. The lower formability limit, on the other hand, was assessed by torsion and tensile-torsion tests in which Fields-Backofen algorithm [10, 11, 12] was used to determine the strain at fracture, while again FE simulation was used to assess triaxiality factor. The fracture locus shape, different if compared with what expected from the original model [9], was explained to be due to the different rheological behavior of the material at high temperatures. SEM fractografic analyses were carried on the fractured surfaces in order to determine the fracture mode, while SEM-EDS analysis was performed to determine grain boundary composition and correlate it to the formability characteristics previously highlighted.

2 EXPERIMENTAL CAMPAIGN

The experimental plan was designed keeping into account the standard process parameters in the hot forging process of the reference brass alloy. In particular the standard process temperature is 700°C and the part is forged in a multistep mechanical press. In order to investigate the formability limits of the material, a lower temperature range was taken: the three temperature 500°C, 650°C and 750°C were chosen. The strain rate range was chosen in the typical values for mechanical presses: $1s^{-1}$, $10s^{-1}$, $50s^{-1}$.

2.1 Compression tests

Compression tests were carried out on the Gleeble 3800^{TM} thermo-mechanical simulator in order to determine the rheological characteristics of the alloy. During the tests, the specimen is heated up by Joule effect due to current flow through it and, after a homogenization dwell time at test temperature, it is compressed between tungsten carbide punches held by the machine jaws. Spot welded K-thermocouples provide temperature measurement, while good lubrication conditions between punches and specimen is attained by means of graphite foils. The machine control automatically arranges the stroke linear speed in order to keep the strain constant to the set value. In Table 1 the compression test parameters are summarized.

Table 1: Compression test parameters

Test parameters	Values
Temperature [°C]	500, 650, 750 ±2
Strain rate [s^{-1}]	1, 10, 50
Dwell time [s]	30
Heating rate [°C/s]	10
Final strain [-]	0.8
Repeatability [-]	2

2.2 Tensile tests

Tensile tests were performed on notched specimens of three different geometries in order to determine the upper formability limit highlighting the influence of varying stress triaxiality factor. Also the tensile tests were carried out on Gleeble 3800™ thermo-mechanical simulator, which has a specific tensile test setup (see Figure 1.a). In Table 2 the tensile test parameters are summarized.

Table 2: Tensile test parameters

Test parameters	Values
Temperature [°C]	500, 650, 750 ±2
Strain rate [s^{-1}]	1, 10, 50
Dwell time [s]	30
Heating rate [°C/s]	10
Final strain [-]	Till fracture
Notch radius [mm]	3, 6, 20
Repeatability [-]	2

2.3 Torsion tests

Simple torsion tests and torsion tests with a super-imposed axial load were carried out in order to determine the lower formability limit. A dedicated torsion test apparatus was used to perform these tests (see Figure 1.b). In Table 3 the torsion test parameters are summarized.

Table 3: Torsion test parameters

Test parameters	Values
Temperature [°C]	500, 650, 750 ±5
Strain rate [s^{-1}]	1
Dwell time [s]	100
Heating rate [°C/s]	10
Final strain [-]	Till fracture
Repeatability [-]	2

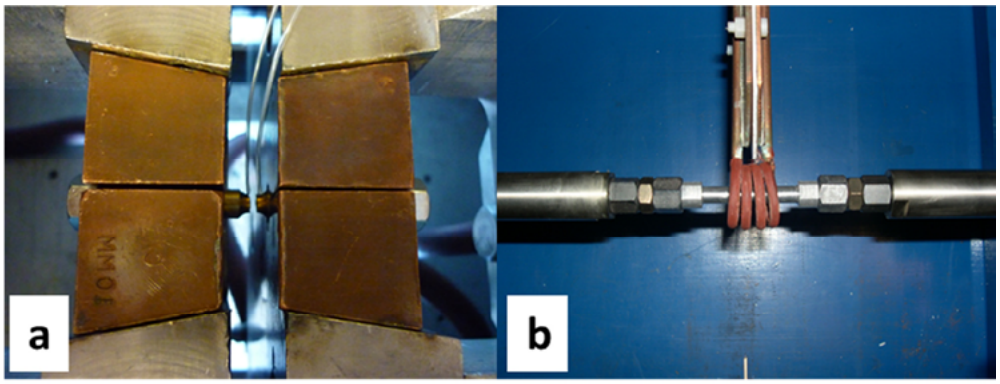

Figure 1: Tensile test setup (a) and torsion test setup (b)

3 RESULTS

3.1 Compression tests

Compression tests results, made available in terms of punch force-punch displacement diagrams, were filtered and elaborated in order to obtain the true stress-true strain curves (see Figure 2).

By means of non-linear regression, the experimental curves were fitted by the simplified Hansel-Spittel model (equation (3)):

$$\sigma = Ae^{m_1 T}\varepsilon^{m_2}\dot{\varepsilon}^{m_3}e^{\left(\frac{m_4}{\varepsilon}\right)} \tag{3}$$

The coefficients obtained in the analyses are displayed in Table 4.

Table 4: Hansel-Spittel's law coefficients

A	m_1	m_2	m_3	m_4
2390	-0.00663	-0.0723	0.1602	-0.01235

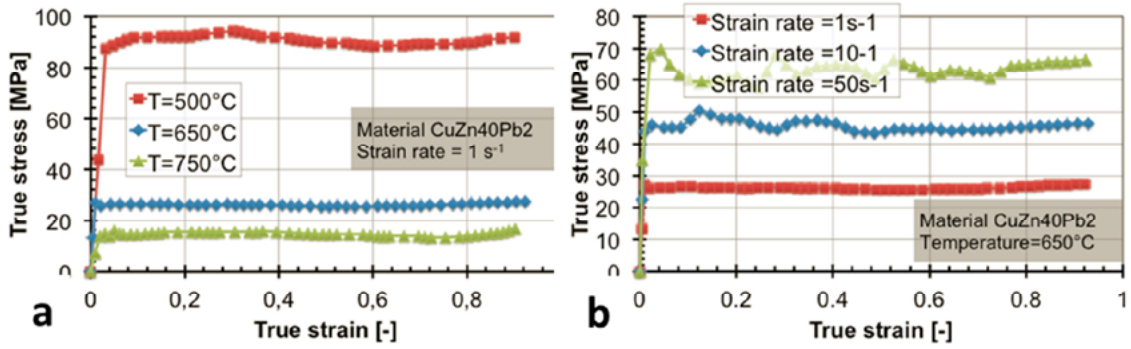

Figure 2**: Flow stress curves: temperature influence (a) and strain rate influence (b)**

3.2 Tensile tests

Tensile tests results were elaborated in order to attain for each test the equivalent strain at fracture and the average stress triaxiality during the deformation. The former was obtained by measuring the cross sectional area of the fractured surface by means of WERTH optical system (see figure 3) and introducing it in equation (4):

$$\varepsilon = ln\left(\frac{A_0}{A_f}\right) \tag{4}$$

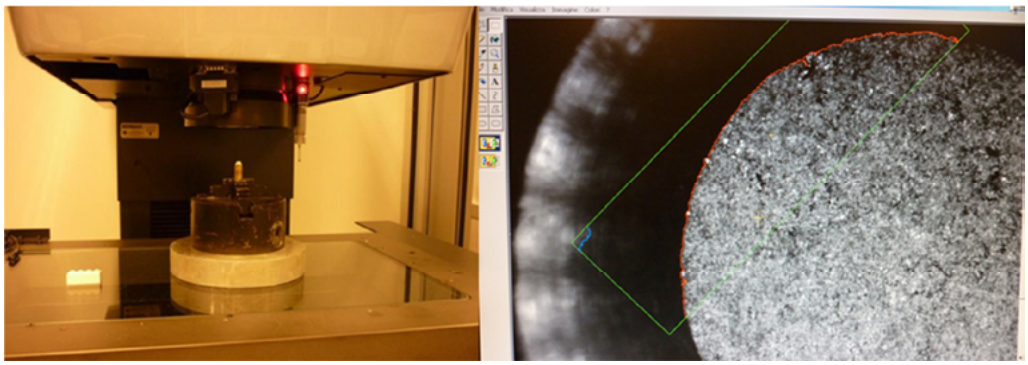

Figure 3: WERTH optical measurement system

The latter was attained by numerical simulation of each tensile test. The results highlighted a negligible influence of strain rate on material formability. In Table 5 the results for strain rate 1 s^{-1} are summarized.

Table 5: Tensile tests results

Temperature [°C]	Notch radius [mm]	Average triaxiality	X	ε_f
500	3	0.86	1	0.090
500	6	0.50	1	0.098
500	20	0.35	1	0.094
650	3	0.89	1	0.274
650	6	0.60	1	0.451
650	20	0.44	1	0.618
750	3	0.88	1	0.893
750	6	0.67	1	1.300
750	20	0.51	1	1.443

3.3 Torsion tests

The torsion testing campaign was performed for the only strain rate 1 s^{-1}. The Fields-Backofen algorithm was applied on the raw test output data (torque-rotation curves) in order to attain a true stress-true strain curve to evaluate the equivalent strain at fracture value needed for the formability model calibration.
Since the values of the equivalent strain at fracture for torsion tests proved to be higher than

those of tensile tests, a complete X=0 limit curve determination was necessary. Thus, a tensile-torsion test was set up applying an axial load to the specimen before torsion: for the test at 500°C an axial load of 200N was applied, while a 150N axial load was used for the two higher temperatures. Once again, FE simulation of the test was used to calculate the average triaxiality factor for each test. In Table 6 results for these tests are summarized.

Table 6: Torsion tests results

Temperature [°C]	Axial load [N]	Average triaxiality	X	ε_f
500	0	0	0	0.44
500	200	0.052	0	0.43
650	0	0	0	1.45
650	150	0.12	0	1.21
750	0	0	0	5.30
750	150	0.22	0	3.99

4 FRACTURE LOCUS DETERMINATION

The formability experimental campaign highlighted that at 500°C the material can bear almost no plastic deformation before rupture, while at 650°C and 750°C the formability of the material rises. For the fracture locus determination, a non-linear regression of equation (2) on experimental data was used. Besides C_1 and C_2 constants values, also n value was interpreted as a model constant to be determined. In Figures 4, 5 and 6 the fracture loci at 750°C, 650°C and 500°C are shown, while in Table 7 are highlighted the coefficients found for the three temperatures examined.

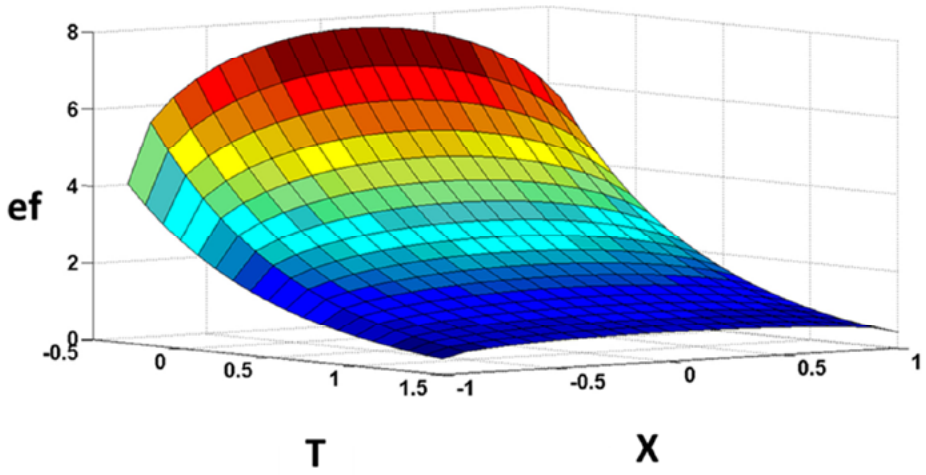

Figure 4: Fracture locus at 750°C

The results show that the fracture locus shape changes if compared with what was found in [7] and [9]. This is essentially due to the fact that the formability limit for the case of plane

strain (X=0) resulted to be higher than that for the case of axisymmetric stress state (X=1). Due to this, the prevision of the X=0 limit using n, the strain hardening coefficient, in the equation (2) is not possible. Indeed this is consistent with the fact that the material was tested at temperatures at which it did not show any strain hardening capability. Moreover the results of the regression show negative values for n, which are consistent with the strain softening behaviour found in the compression tests which corresponds to the negative sign of the m_2 coefficient of the Hansel-Spittel model (see equation (3) and Table 3).

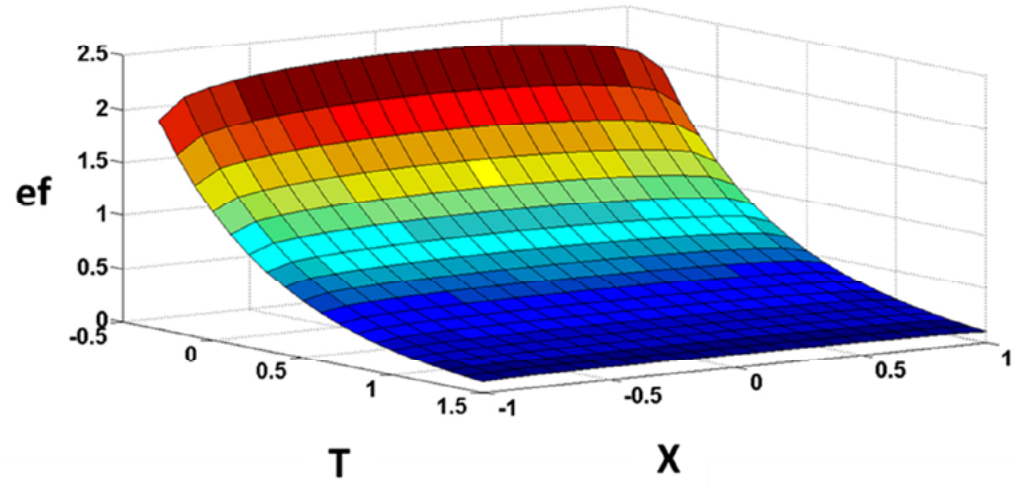

Figure 5: Fracture locus at 650°C

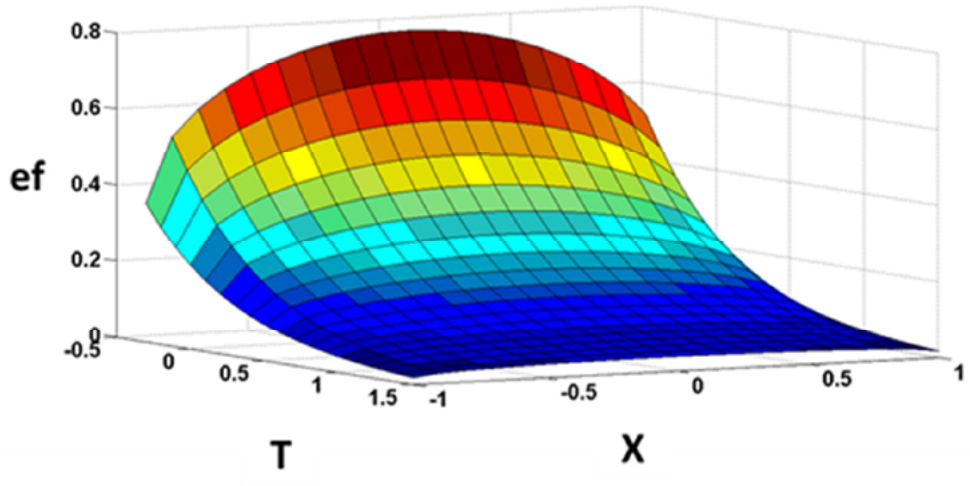

Figure 6: Fracture locus at 500°C

In Table 7 are exposed the coefficients found by regression for the definition of the three fracture loci.

Table 7: Fracture loci coefficients

Temperature [°C]	C_1	C_2	n
500	0,218545	1,683325	-0,18819
650	1,204221	1,636868	-0,77446
750	2,795802	1,296804	-0,2249

5 MICROGRAPHIC AND FRACTOGRAPHIC ANALYSIS

In Figure 7 are shown optical micrographs performed on tensile specimen with notch radius 6mm at the three test temperatures.

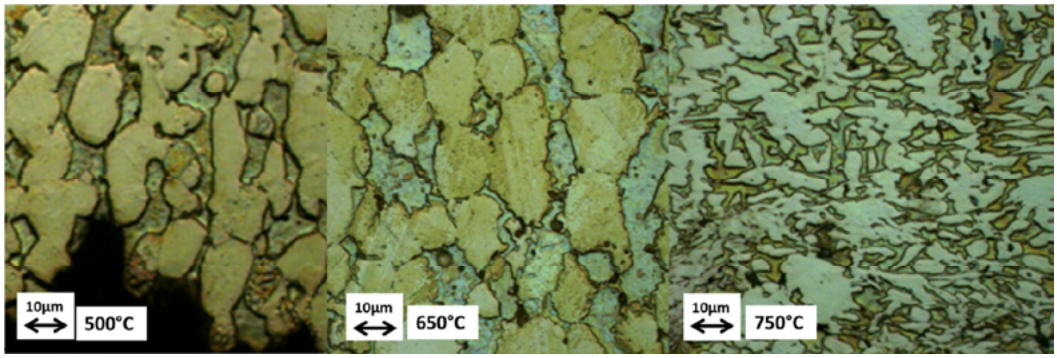

Figure 7: Optical micrographies

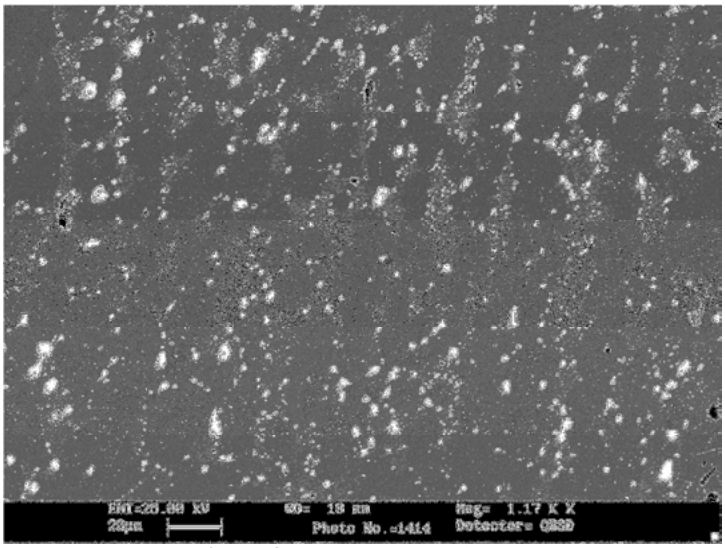

Figure 8: SEM-EDS scansion

The pictures are taken from the deformed zone in proximity of the fracture surface. The two phases composing the alloy can be clearly distinguished. It can be noticed how at the highest temperature the grains shape is very irregular, probably due to the very high strain levels reached. As also proved by SEM-EDS, the dark zones at the grain boundaries are lead drops which are not soluble in the two main phases and deposite at the grain boundaries being the cause of the brittle fracture at the lowest temperature investigated. In Figure 8 it is shown a picture of the SEM-EDS analysis which clearly highlights the lead deposition at the grain boundaries (white zones).

6 CONCLUSIONS

- An experimental campaign of mechanical and formability characterization by means of compression, tensile and torsion tests was performed on a dual-phase brass alloy used in hot forging industrial processes.
- The calibration of a damage criterion was made and the fracture loci for the three temperature tested were found.
- It was highlighted how the unexpected fracture locus shape is seemingly due to different rheological characteristics of the material at high temperatures.
- Microstructure and fractography analyses highlighted that the reason for the formability drop which was noticed between 650°C and 500°C is the presence of lead at the grain boundaries.

REFERENCES

[1] M. G. Cockroft, D. J. Latham, Ductility and the Workability of Metals. *J. Inst. Met.* (1968) **96**:33.
[2] J. R. Rice, D. M. Tracey, On the Ductile Enlargement of Voids in Triaxial Stress Fields. *J Mech Phys Solids* (1969) **17**:201.
[3] M. Oyane, Criteria For Ductile Fracture Strain. *Bull. JSME* (1972) **15**:1507.
[4] J. Lemaitre, R. Desmorat, *Engineering Damage Mechanics.* Springer-Verlag, Berlin (2005).
[5] Y. Bao, T. Wierzbicki, On fracture locus in the equivalent strain and stress triaxiality space. *International Journal of Mechanical Sciences* (2004) **46**: 81-98.
[6] T. Wierzbicki, Y. Bao, Y. W. Lee, Y. Bai, Calibration and evaluation of seven fracture models. *International Journal of Mechanical Sciences* (2005) **47**: 719-743.
[7] T. Coppola, L. Cortese, P. Folgarait, The effect of stress invariants on ductile fracture limit in steels. *Engineering Fracture Mechanics* (2009) **76**: 1288-1302.
[8] L. Xue, Damage accumulation and fracture initiation in uncracked ductile solids subject to triaxial loading. *International Journal of Solids and Structures* (2007) **44**: 5163-5181.
[9] P. F. Bariani, S. Bruschi, A. Ghiotti, M. Simionato, Ductile fracture prediction in cold forging process chains. *CIRP Annals – Manufacturing Technology* (2011) **60/1**: 287-290.
[10] A. Nadai, *Theory of Flow and Fracture of Solids*. Engineering Societies Monographs, Vol. I, (1950).
[11] D. S. Fields, W. A. Backofen, Determination of strain-hardening characteristics by torsion testing. *Proceedings of the 6th annual meeting of the society J ASTM* (1957) **57**: 1259-1272.

[12] G. E. Dieter, H. A. Kuhn, S. L. Semiatin, *Handbook of Workability and Process Design*. ASM International, (2003).